Probing the $\mathcal{O}(1/\Lambda^4)$ SMEFT Effects in the Drell-Yan process at LHC

Yingsheng Huang

Northwestern U. & Argonne

In collaboration with:

Radja Boughezal and **Frank Petriello**

Northwestern University

May 10th @ Phenomenology 2022

Table of contents

Introduction

Status of the SM

Examples:

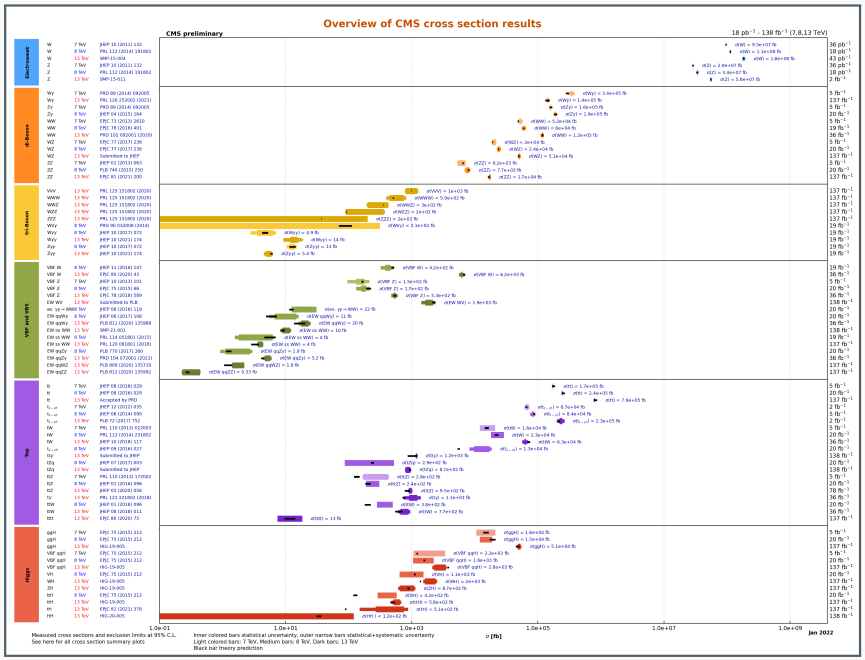

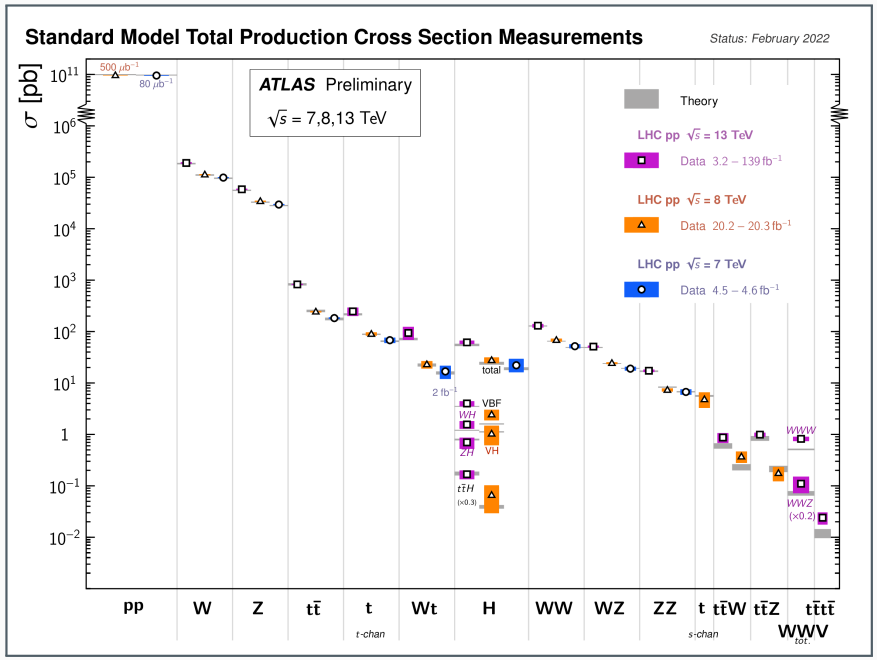

Remarkable agreement between theory predictions and the experiment measurements!

BSM SEARCHES

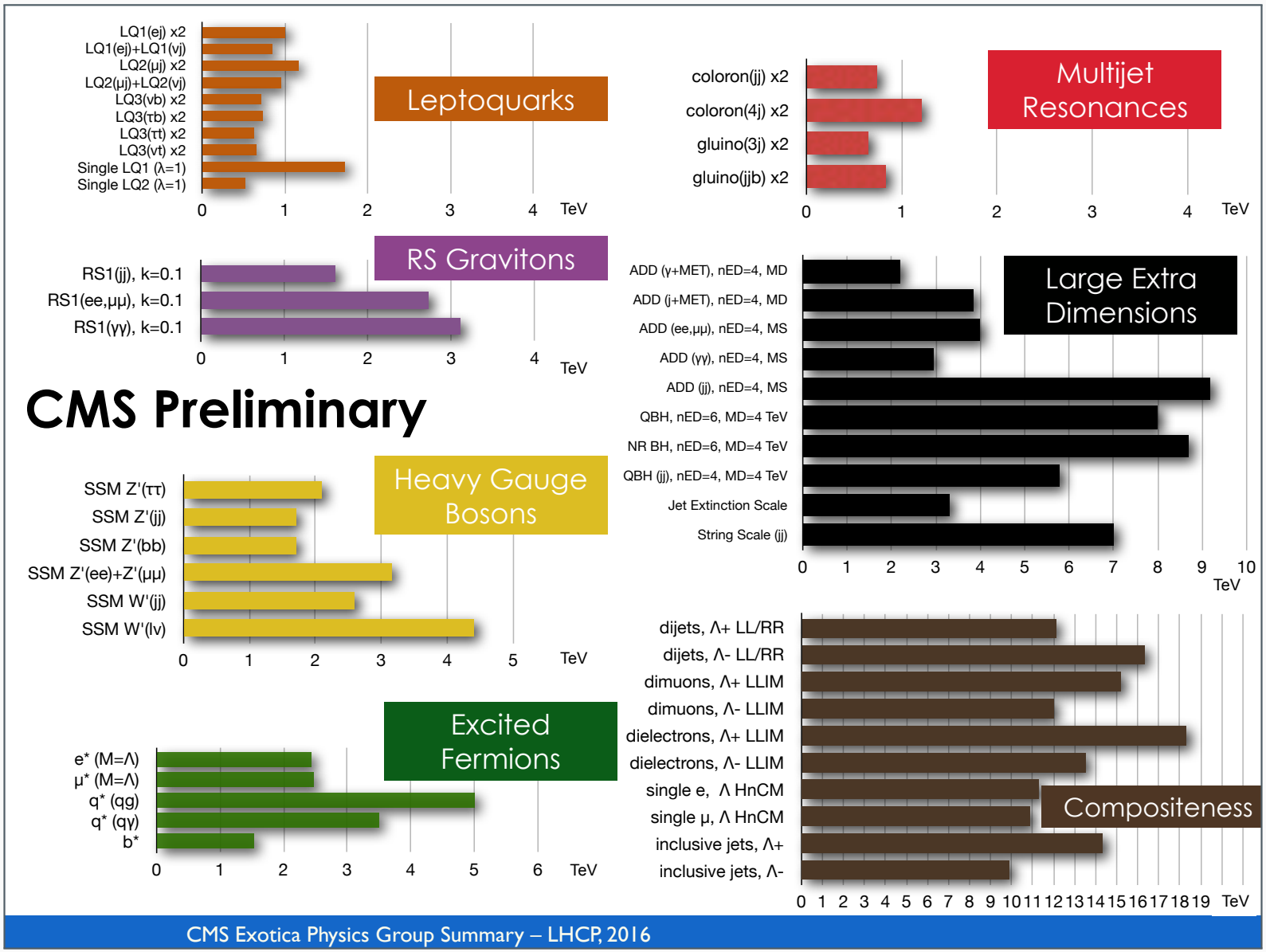

SMEFT a model-independent approach

- No BSM particle found
- Calls for precision test of SM

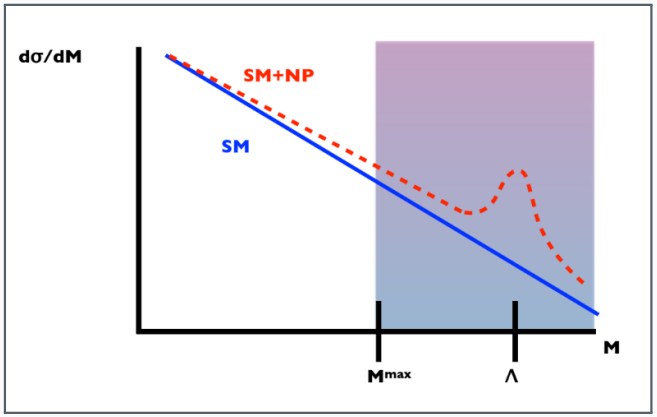

SMEFT a model-independent approach

- No BSM particle found
- Calls for precision test of SM

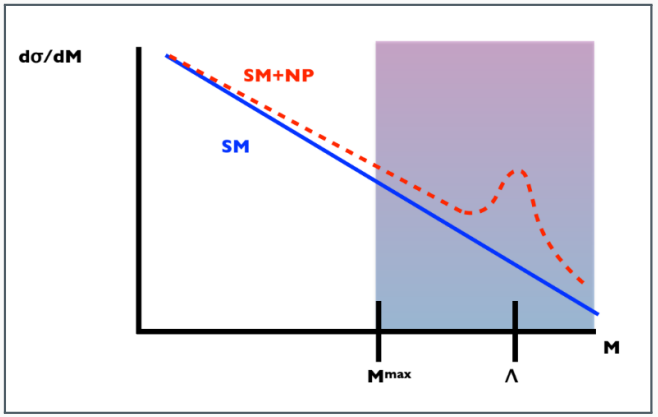

- Standard Model Effective Field Theory (SMEFT)
  - SM particles
  - all possible operators satisfying symmetries of the SM
  - power counting: new physics scale Λ

SMEFT a model-independent approach

- No BSM particle found
- Calls for precision test of SM

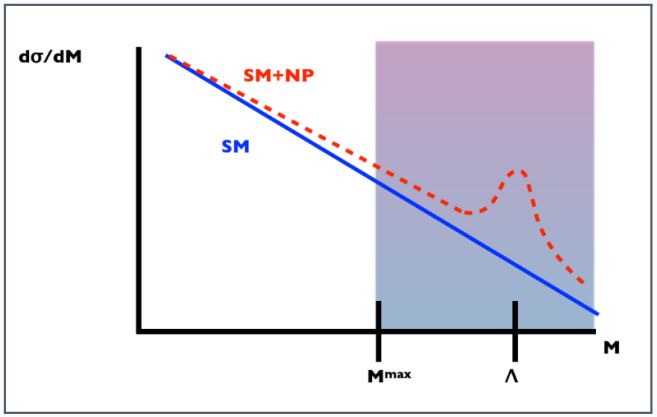

- Standard Model Effective Field Theory (SMEFT)
  - SM particles
  - all possible operators satisfying symmetries of the SM
  - power counting: new physics scale Λ

$$\mathcal{L}_{\text{SMEFT}} = \mathcal{L}_{\text{SM}} + \boxed{\frac{1}{\Lambda^2}\sum C_6\mathcal{O}_6} + \boxed{\frac{1}{\Lambda^4}\sum C_8\mathcal{O}_8} + \cdots$$

  - No odd dimensions in this talk
  - ▶ $\boxed{\mathcal{L}_6}$: 76 B-preserving Lagrangian terms, 2499 parameters **Grzadkowski et al. 2010**
  - ▶ $\boxed{\mathcal{L}_8}$: 1031 Lagrangian terms, 44807 parameters **Murphy 2020; Li et al. 2021**
- No specific model needed

SMEFT a model-independent approach

- No BSM particle found
- Calls for precision test of SM

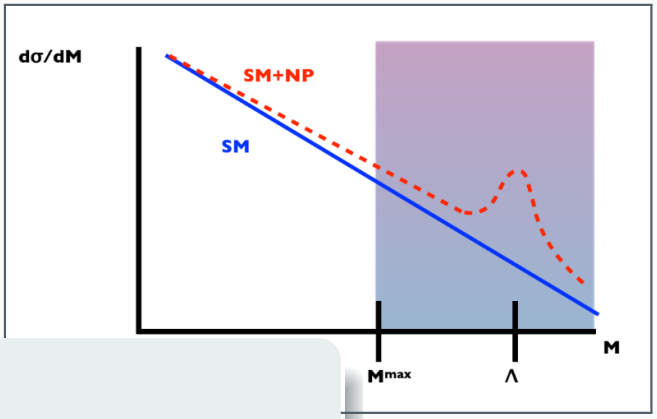

- Standard M
  - SM par
  - all pos
  - power

In this talk:

Warsaw basis for dimension-6

Murphy's basis for dimension-8

$$\mathcal{L}_{\text{SMEFT}} = \mathcal{L}_{\text{SM}} + \frac{1}{\Lambda^2}\sum C_6\mathcal{O}_6 + \frac{1}{\Lambda^4}\sum C_8\mathcal{O}_8 + \cdots$$

  - No odd dimensions in this talk
  - ▶ $\mathcal{L}_6$: 76 B-preserving Lagrangian terms, 2499 parameters **Grzadkowski et al. 2010**
  - ▶ $\mathcal{L}_8$: 1031 Lagrangian terms, 44807 parameters **Murphy 2020; Li et al. 2021**
- No specific model needed

MOTIVATION for the inclusion of dimension-8 operators

- How important are the dim-8 effects at LHC?

- How sensitive are current fits to the dim-8 effects?

We'll investigate those questions using LHC Drell-Yan data as an example:

- dilepton invariant mass spectrum **Boughezal, Mereghetti and Petriello, 2106.05337**
- dilepton double differential distribution (m_{ll} and p_T)
  will address as p_T spectra in this talk **Boughezal YH, and Petriello to appear**

Dilepton invariant mass spectra

Experimental measurements 1606.01736

- Probe high m_{ll}
  Up to $1.5\ \mathrm{TeV}$
- 12 m_{ll} bins:
  [116,130,150,175,200,
  230,260,300,380,500,
  700,1000,1500]

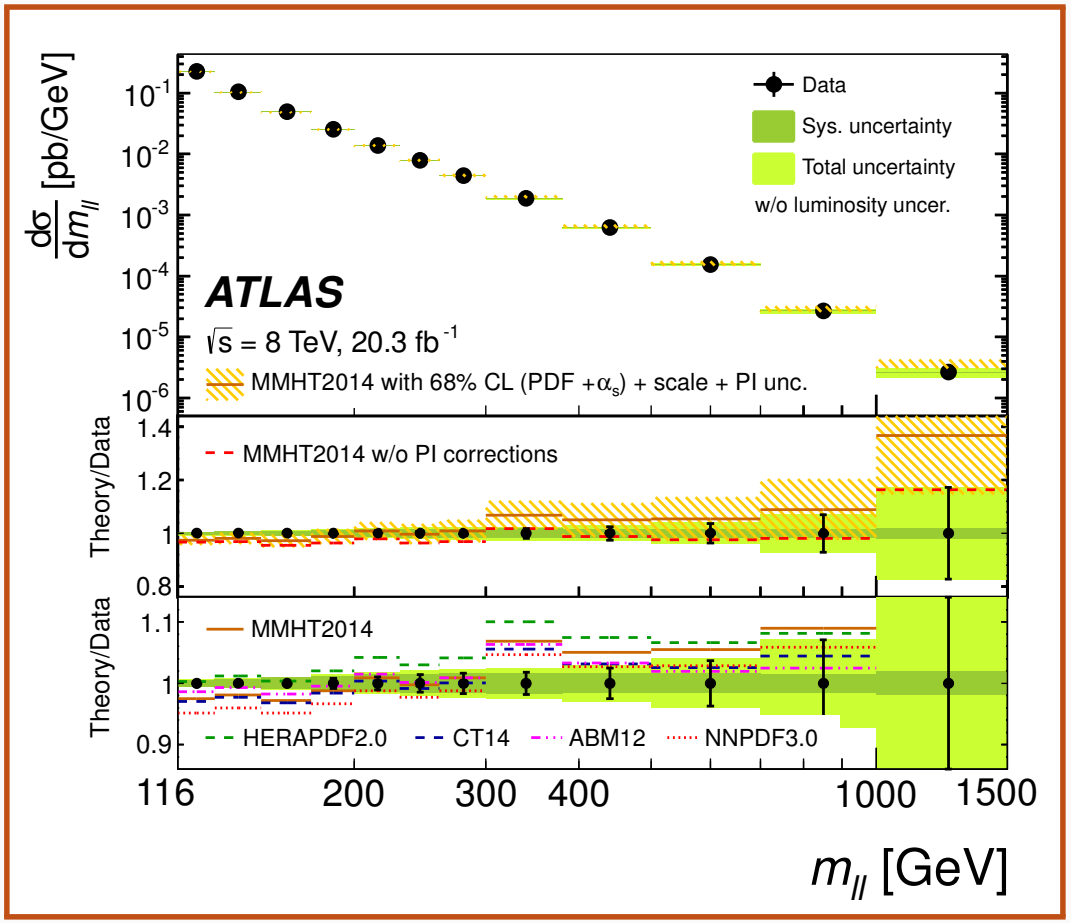

Relevant operators dimension-6

- Study scaling of cross sections in high energy limit (s, v)
- Only show some examples for each category
- q, l: left-handed fermion doublets

  e, u, d: right-handed fermion singlets

  ϕ: Higgs doublet

$\mathcal{L}_{\psi^2 X^2 \phi}$

$$\frac{C_{eB}}{\Lambda^2}\bar{l}\sigma^{\mu\nu}B_{\mu\nu}\phi e$$

$$\frac{C_{uW}}{\Lambda^2}\bar{q}\sigma^{\mu\nu}\tau^I W^I_{\mu\nu}\phi u$$

Dipole coupling

assume massless fermion

$\sim \mathcal{O}(v^2 s/\Lambda^4)$

$\mathcal{L}_{\psi^2 \phi^2 D}$

$$\frac{C^{(1)}_{Hl}}{\Lambda^2}\phi^\dagger \overleftrightarrow{D^\mu}\phi\bar{l}\gamma_\mu l$$

$$\frac{C_{Hu}}{\Lambda^2}\phi^\dagger \overleftrightarrow{D^\mu}\phi\bar{u}\gamma_\mu u$$

Z-vertex corrections

$\sim \mathcal{O}(v^2/\Lambda^2)$

$\mathcal{L}_{\psi^4}$

$$\frac{C^{(1)}_{lq}}{\Lambda^2}\bar{l}\gamma^\mu l q\gamma_\mu q$$

$$\frac{C_{ld}}{\Lambda^2}\bar{l}\gamma^\mu l d\gamma_\mu d$$

Four-fermion interactions

$\sim \mathcal{O}(s/\Lambda^2)$

RELEVANT OPERATORS dimension-8 four-fermion

- Study scaling of cross sections in high energy limit (s, v)
- Only show some examples for each category
- q, l: left-handed fermion doublets

  e, u, d: right-handed fermion singlets

  ϕ: Higgs doublet

$\mathcal{L}_{\psi^4 D^2}$

$$\frac{C^{(1)}_{l^2 q^2 D^2}}{\Lambda^4} \partial_\nu \left(\bar{l}\gamma^\mu l\right) \partial^\nu \left(\bar{q}\gamma_\mu q\right)$$

$$\frac{C^{(1)}_{l^2 d^2 D^2}}{\Lambda^4} \partial_\nu \left(\bar{l}\gamma^\mu l\right) \partial^\nu \left(\bar{d}\gamma_\mu d\right)$$

Momentum-dependent four-fermion interactions

$\sim \mathcal{O}(s^2/\Lambda^4)$

$\mathcal{L}_{\psi^4 H^2}$

$$\frac{C^{(1)}_{l^2 q^2 H^2}}{\Lambda^4} \left(\bar{l}\gamma^\mu l\right) \left(\bar{q}\gamma_\mu q\right) \phi^\dagger \phi$$

$$\frac{C^{(1)}_{l^2 d^2 H^2}}{\Lambda^4} \left(\bar{l}\gamma^\mu l\right) \left(\bar{d}\gamma_\mu d\right) \phi^\dagger \phi$$

Momentum-independent four-fermion interactions

$\sim \mathcal{O}(v^2 s/\Lambda^4)$

RELEVANT OPERATORS dimension-8 Z-vertex corrections

- Study scaling of cross sections in high energy limit (s, v)
- Only show some examples for each category
- q, l: left-handed fermion doublets

  e, u, d: right-handed fermion singlets

  ϕ: Higgs doublet

$\mathcal{L}_{\psi^2 D^3}$

$$\frac{C^{(1)}_{l^2 H^2 D^3}}{\Lambda^4} i\bar{l}\gamma^\mu D^\nu l \left(D_{(\mu} D_{\nu)}\phi\right)^\dagger \phi$$

$$\frac{C^{(3)}_{q^2 H^2 D^3}}{\Lambda^4} i\bar{q}\gamma^\mu \tau^I D^\nu q \left(D_{(\mu} D_{\nu)}\phi\right)^\dagger \tau^I \phi$$

Momentum-dependent Z-vertex corrections

$$\sim \mathcal{O}(v^2 s/\Lambda^4)$$

$\mathcal{L}_{\psi^2 H^4 D}$

$$\frac{C^{(1)}_{l^2 H^4 D}}{\Lambda^4} i \left(\bar{l}\gamma^\mu l\right) \left(\phi^\dagger \overleftrightarrow{D}_\mu \phi\right) \left(\phi^\dagger \phi\right)$$

$$\frac{C^{(1)}_{u^2 H^4 D}}{\Lambda^4} i \left(\bar{u}\gamma^\mu u\right) \left(\phi^\dagger \overleftrightarrow{D}_\mu \phi\right) \left(\phi^\dagger \phi\right)$$

Momentum-independent Z-vertex corrections

$$\sim \mathcal{O}(v^4/\Lambda^4)$$

SMEFT CROSS SECTIONS

Structure of the SMEFT cross section

$$\frac{\mathrm{d}\sigma}{\mathrm{d}m_{\ell\ell}} = \frac{\mathrm{d}\sigma_{\mathrm{SM}}}{\mathrm{d}m_{\ell\ell}} + \sum_i \left(\frac{a_i^{(6)}(m_{\ell\ell})}{\Lambda^2} C_i^{(6)} + \frac{a_i^{(8)}(m_{\ell\ell})}{\Lambda^4} C_i^{(8)} \right) + \sum_{i,} \frac{b_{ij}^{(6)}(m_{\ell\ell})}{\Lambda^4} C_i^{(6)} C_j^{(6)}$$

- a_i, b_{ij} terms: NLO QCD corrections included (30%)
- SM: NNLO in QCD, NLL Sudakov logs through $\mathcal{O}(\alpha_s)$
- $\Lambda = 4\ \mathrm{TeV} \gg 1.5\ \mathrm{TeV}$ (the m_{ll} upper bound of the dataset)
- Complete to $\mathcal{O}(\alpha_s/\Lambda^2)$
  Complete to $\mathcal{O}(1/\Lambda^4)$
  at $\mathcal{O}(\alpha_s/\Lambda^4)$: missing $\psi^4 G$-type operators

Impact of dim-6/8 terms

Boughezal, Mereghetti and Petriello
2106.05337

- ψ^4: C_{eu}, C_{lu}
- Consider linear a_i terms $(1/\Lambda^2)$ and quadratic b_{ii} terms $(1/\Lambda^4)$
- Quadratic terms: 50% (C_{eu}) or 100% (C_{lu}) in $1 - 1.5$ TeV bin

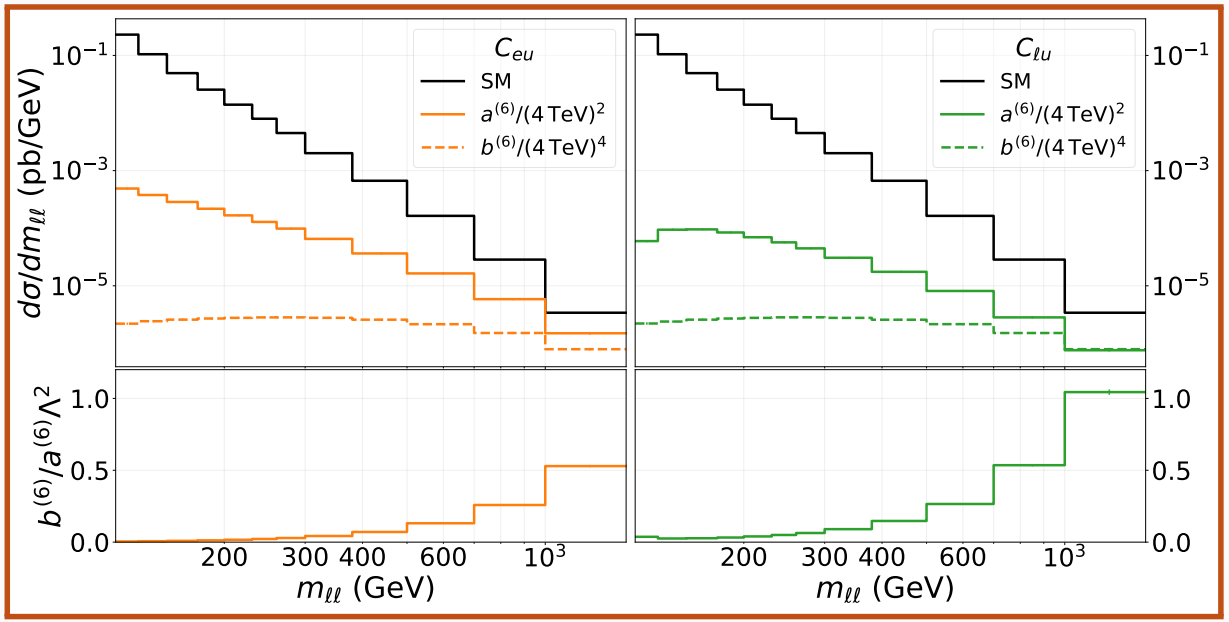

- $\psi^4 D^2$-type: $C_{e^2 u^2 D^2}$
  $\psi^4 H^2$-type: $C_{e^2 u^2 H^2}$
  $\psi^2 D^3$-type:
  $C_{e^2 H^2 D^3}$, $C_{u^2 H^2 D^3}$
- dim-8 terms: major contribution from $\psi^4 D^2$-type

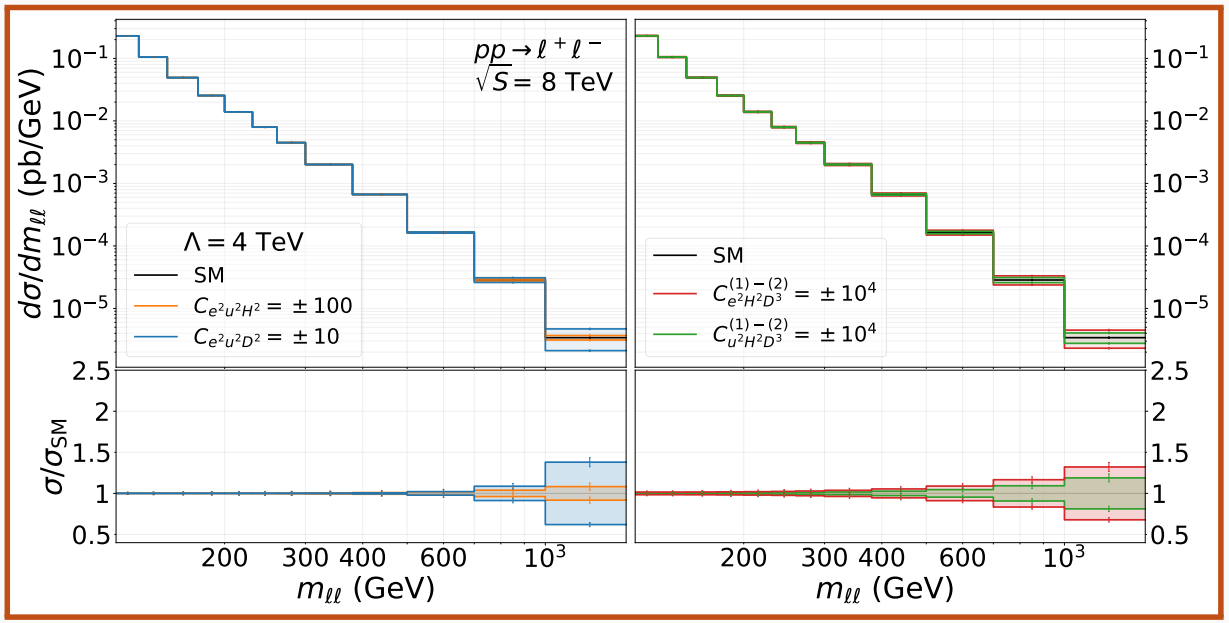

SINGLE-COUPLING FITS dim-6 four-fermion

Boughezal, Mereghetti and Petriello
2106.05337

- Turn on one coupling at a time
- Experimental error matrix; **1606.01736** NNPDF 3.1 PDF errors; NLO QCD scale variation errors

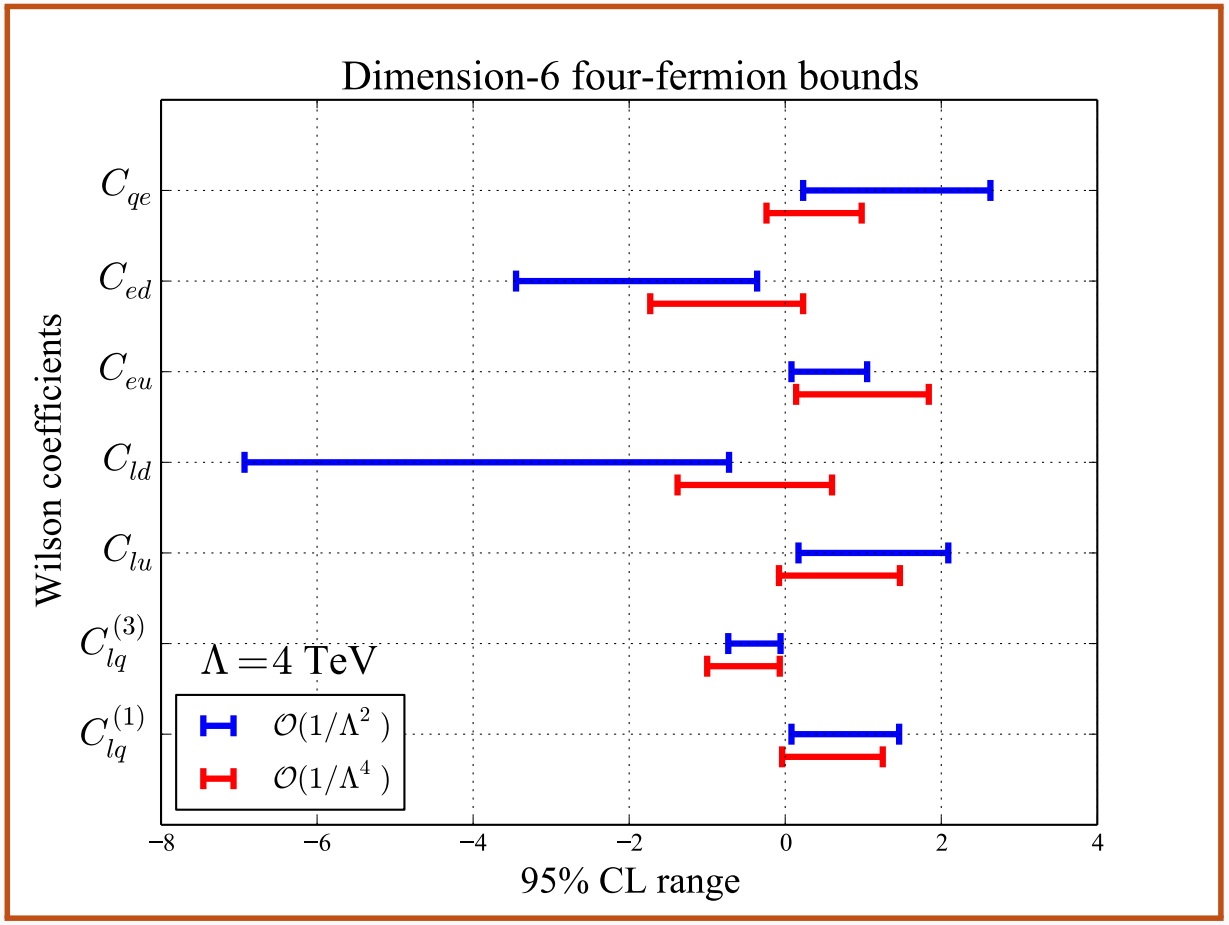

- effective scale $\Lambda/\sqrt{C} \sim 4 \text{ TeV} \gg 1.5 \text{ TeV}$
- Large shift from $1/\Lambda^4$ effects: factors of 2-3 for C_{qe}, C_{ld}

$\mathcal{O}(1/\Lambda^4)$ EFFECTS

Boughezal, Mereghetti and Petriello
2106.05337

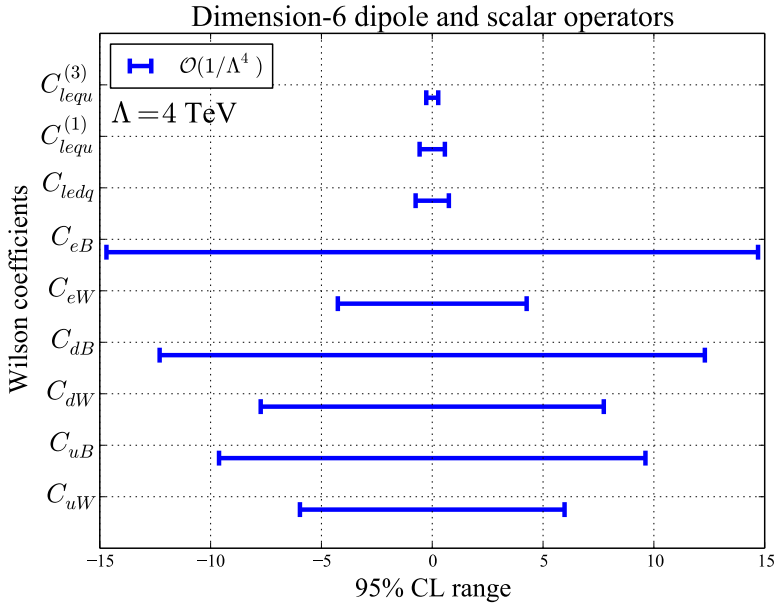

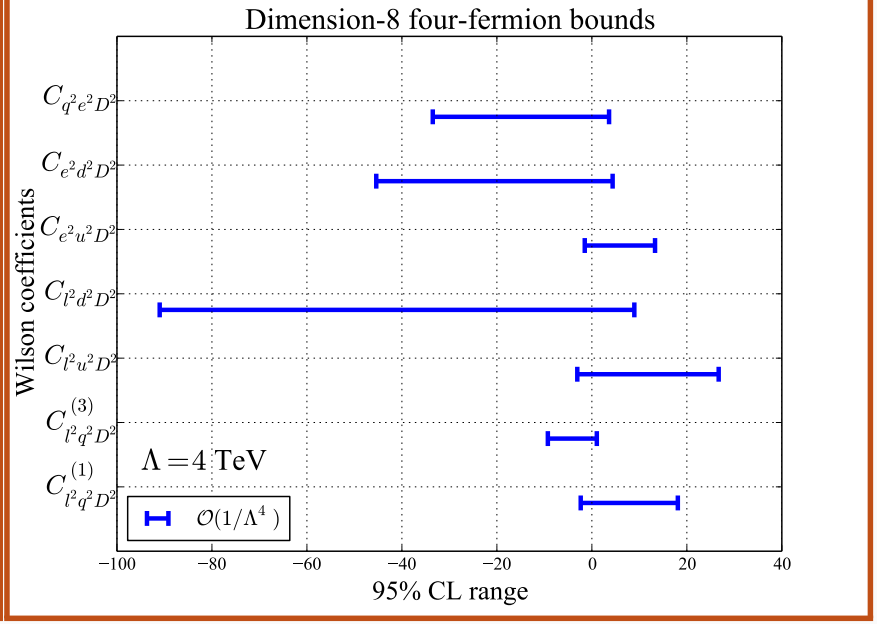

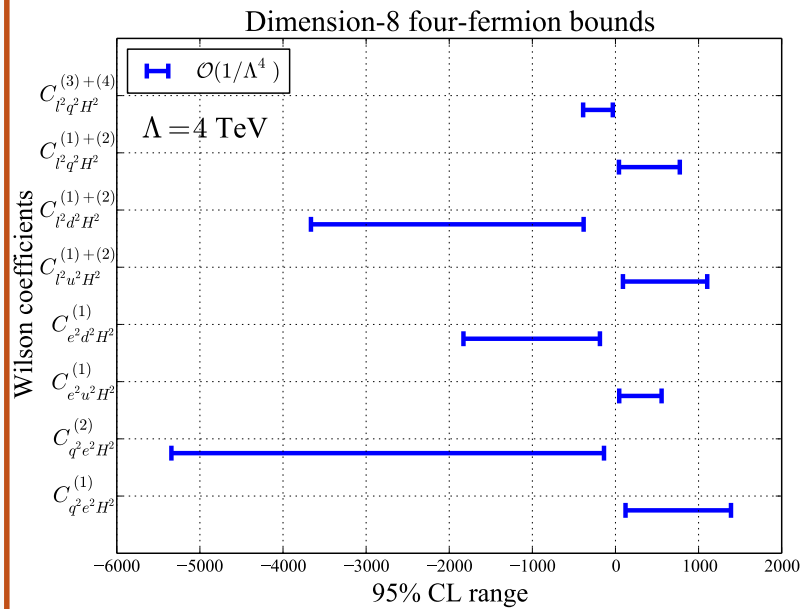

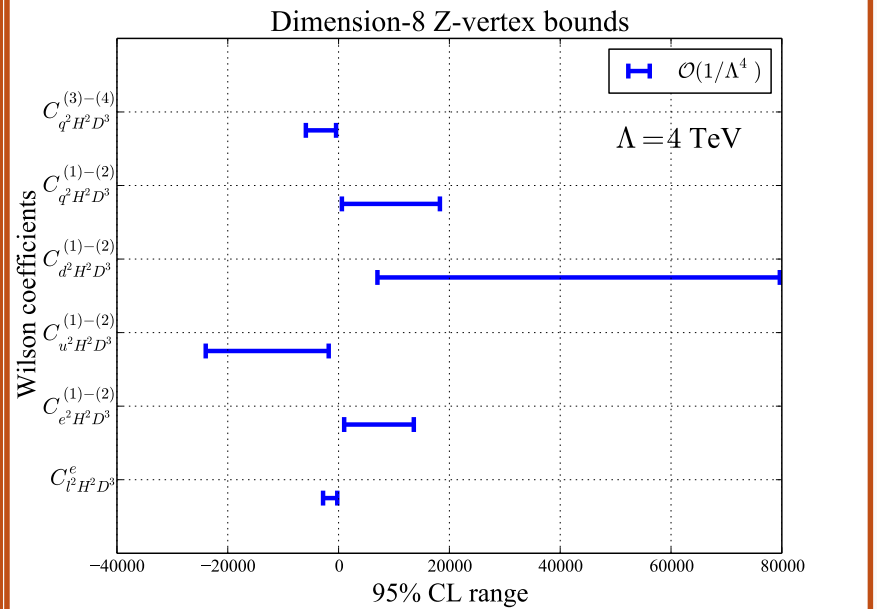

$\mathcal{O}(1/\Lambda^4)$ EFFECTS

Boughezal, Mereghetti and Petriello
2106.05337

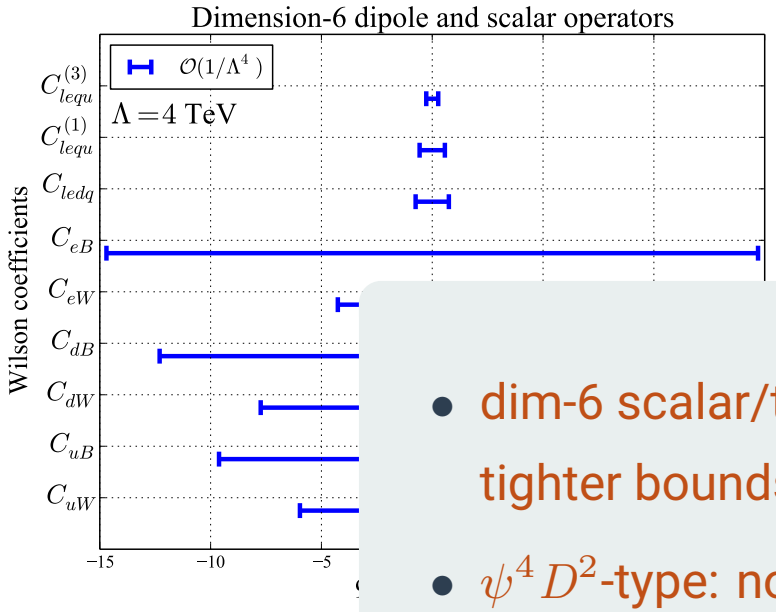

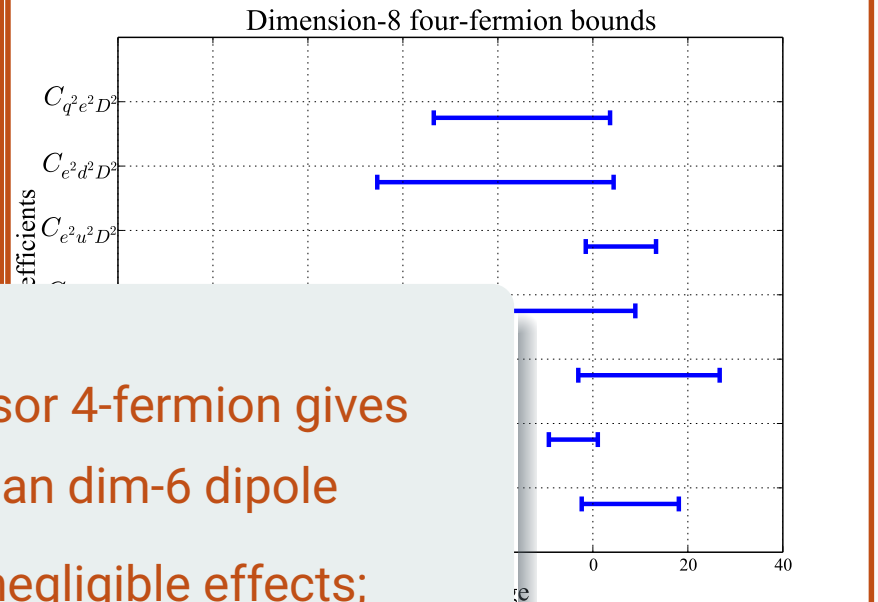

- dim-6 scalar/tensor 4-fermion gives tighter bounds than dim-6 dipole
- $\psi^4 D^2$-type: non-negligible effects; effective scale ~ 2 TeV
- $\psi^4 H^2$ & Z-vertex: negligible

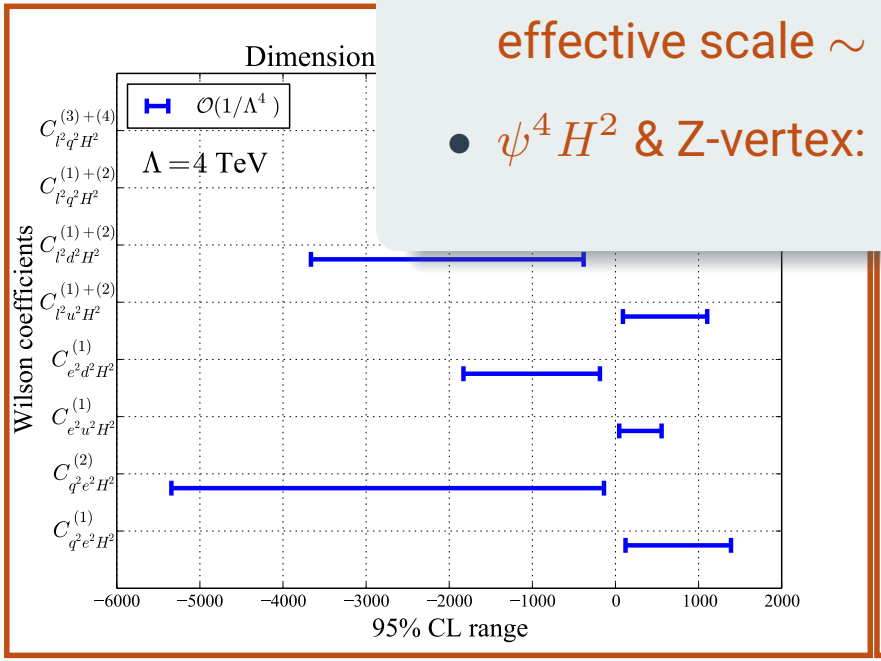

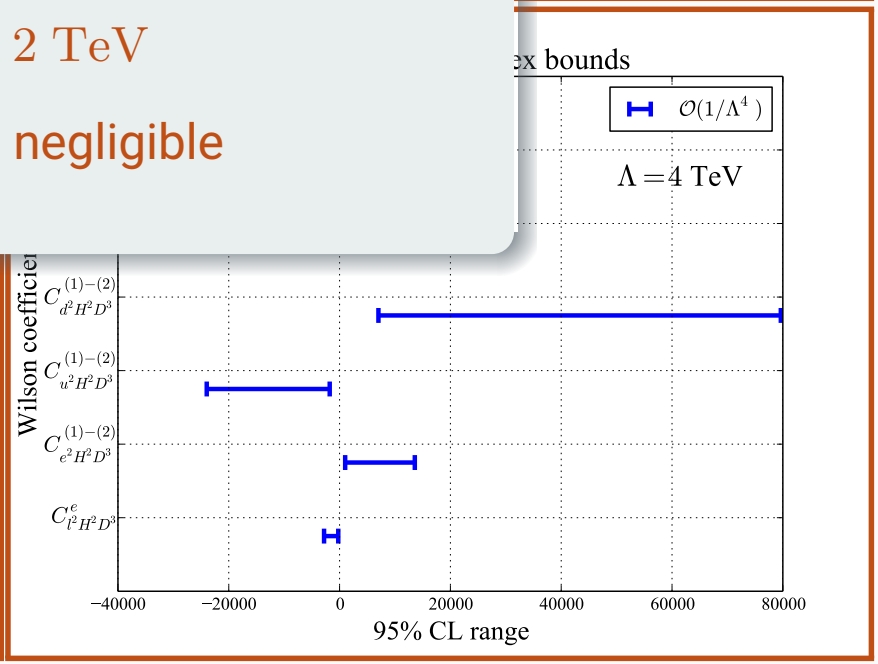

MULTI-COUPLING FITS

Boughezal, Mereghetti and Petriello
2106.05337

	dim-6	single coupling	marginalized	marginalized*
C_{eu}	$[\mathbf{0.08}, \mathbf{1.0}]$	$[\mathbf{0.1}, \mathbf{1.8}]$	$[-39, 39]$	$[\mathbf{-0.6}, \mathbf{2.4}]$
$C_{e^2u^2D^2}$	–	$[-1.5, 13]$	$[-17, 9.2 \cdot 10^3]$	$[-14, 18]$
$C_{e^2u^2H^2}$	–	$[45, 555]$	$[-1.9, 1.2] \cdot 10^4$	$[-256, 256]$
$C^{(1)-(2)}_{u^2H^2D^3}$	–	$[-24, -1.8] \cdot 10^3$	$[-1.2, 1.8] \cdot 10^5$	$[-256, 256]$

- dim-6: Turn on one coupling at a time, only include $\mathcal{O}(1/\Lambda^2)$
- single coupling: Turn on one coupling at a time, include $\mathcal{O}(1/\Lambda^4)$
- marginalized: Turn on all couplings
- marginalized*: Turn on all couplings, and demand effective scale greater than $1\ \mathrm{TeV}$ for last two operators

Bounds on dim-6 Wilson coefficient significantly weakened by turning on dim-8 operators

Dilepton mass-dependent p_T spectra

Boughezal, YH, and Petriello, to appear

Dilepton mass-dependent p_T spectra with CMS data

EXPERIMENTAL MEASUREMENTS ratio to peak region CMS-PAS-SMP-20-003

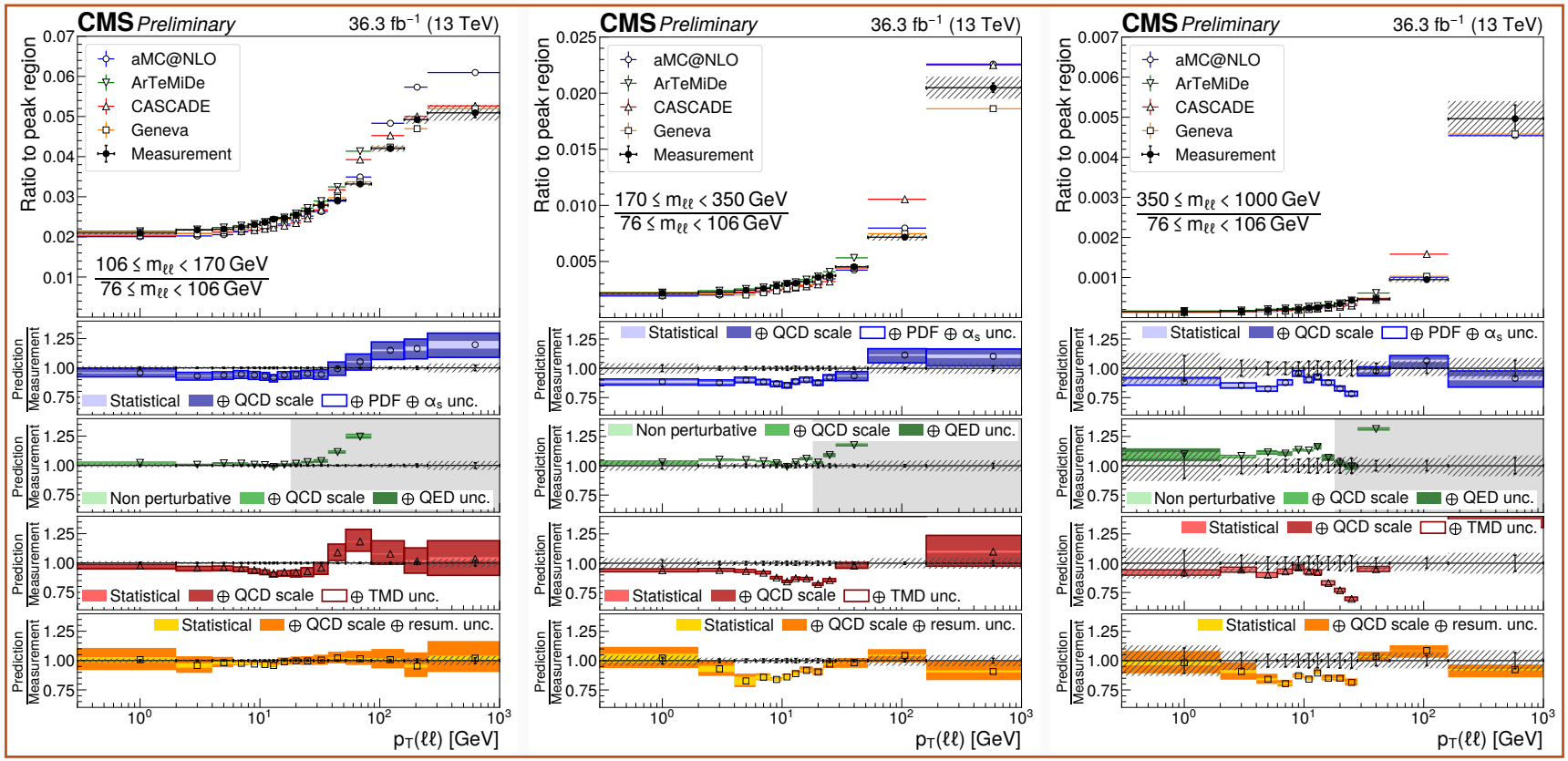

- Ratios of differential unfolded cross sections in $p_T(ll)$ for invariant mass ranges with respect to the peak region $76 < m_{ll} < 106$ GeV
- ~~$50 < m_{ll} < 76$ GeV~~ $106 < m_{ll} < 170$ GeV (left)
  $170 < m_{ll} < 350$ GeV (center) $350 < m_{ll} < 1000$ GeV (right)
- Smaller uncertainties than the cross sections
- We'll use the last 3 m_{ll} bins as the experimental dataset

Most relevant operators

- Study scaling of cross sections in high energy limit, only highest in s
- Only show some examples for each category
- q, l: left-handed fermion doublets

  e, u, d: right-handed fermion singlets

  ϕ: Higgs doublet, G: Gluon field strength tensor

$\mathcal{L}_{\psi^4}$	$\mathcal{L}_{\psi^4 D^2}$	$\mathcal{L}_{\psi^4 G}$
$\frac{C_{eu}}{\Lambda^2}(\bar{e}\gamma^\mu e)(\bar{u}\gamma_\mu u)$	$\frac{C^{(1)}_{e^2u^2D^2}}{\Lambda^4} D^\nu (\bar{e}\gamma^\mu e)\, D_\nu (\bar{u}\gamma_\mu u)$	$\frac{C^{(1)}_{e^2u^2G}}{\Lambda^4} (\bar{e}\gamma^\mu e)\,(\bar{u}\gamma^\nu T^a u)\, G^a_{\mu\nu}$
$\frac{C_{qe}}{\Lambda^2}(\bar{q}\gamma^\mu q)(\bar{e}\gamma_\mu e)$	$\frac{C^{(1)}_{q^2e^2D^2}}{\Lambda^4} D^\nu (\bar{q}\gamma^\mu q)\, D_\nu (\bar{e}\gamma_\mu e)$	$\frac{C^{(1)}_{l^2q^2G}}{\Lambda^4} (\bar{q}\gamma^\mu T^a q)\,(\bar{l}\gamma_\nu l)\, G^a_{\mu\nu}$
Four-fermion interactions	Momentum-dependent four-fermion interactions	Four-fermion interactions with gluon field strength tensor
$\sim \mathcal{O}(s/\Lambda^2)$	$\sim \mathcal{O}(s^2/\Lambda^4)$	$\sim \mathcal{O}(s^2/\Lambda^4)$

SMEFT CROSS SECTIONS

Structure of the SMEFT cross section

$$\frac{\mathrm{d}\sigma}{\mathrm{d}p_T(\ell\ell)} = \frac{\mathrm{d}\sigma_{\mathrm{SM}}}{\mathrm{d}p_T} + \sum_i \left(\frac{a_i^{(6)}(p_T)}{\Lambda^2} C_i^{(6)} + \frac{a_i^{(8)}(p_T)}{\Lambda^4} C_i^{(8)} \right) + \sum_{i,} \frac{b_{ij}^{(6)}(p_T)}{\Lambda^4} C_i^{(6)} C_j^{(6)}$$

- Choose 3 operators (involving right-handed quarks and leptons) as example:

  Q_{eu}: $\frac{C_{eu}}{\Lambda^2}(\bar{e}\gamma^\mu e)(\bar{u}\gamma_\mu u)$

  $Q^{(1)}_{e^2u^2D^2}$: $\frac{C^{(1)}_{e^2u^2D^2}}{\Lambda^4} D^\nu (\bar{e}\gamma^\mu e) D_\nu (\bar{u}\gamma_\mu u)$

  $Q^{(2)}_{e^2u^2G}$: $\frac{C^{(2)}_{e^2u^2G}}{\Lambda^4} (\bar{e}\gamma^\mu e)(\bar{u}\gamma^\nu T^a u) \tilde{G}^a_{\mu\nu}$
- SM: NLO QCD
- SMEFT corrections: LO
- $\Lambda = 2\ \mathrm{TeV}$

Impact of dim-6 terms

- p_T bins: $50\ \mathrm{GeV}$ constant bin widths
- Largest corrections to the ratio
- 10-30% for the highest m_{ll} bin
- Slowest increase as p_T goes higher

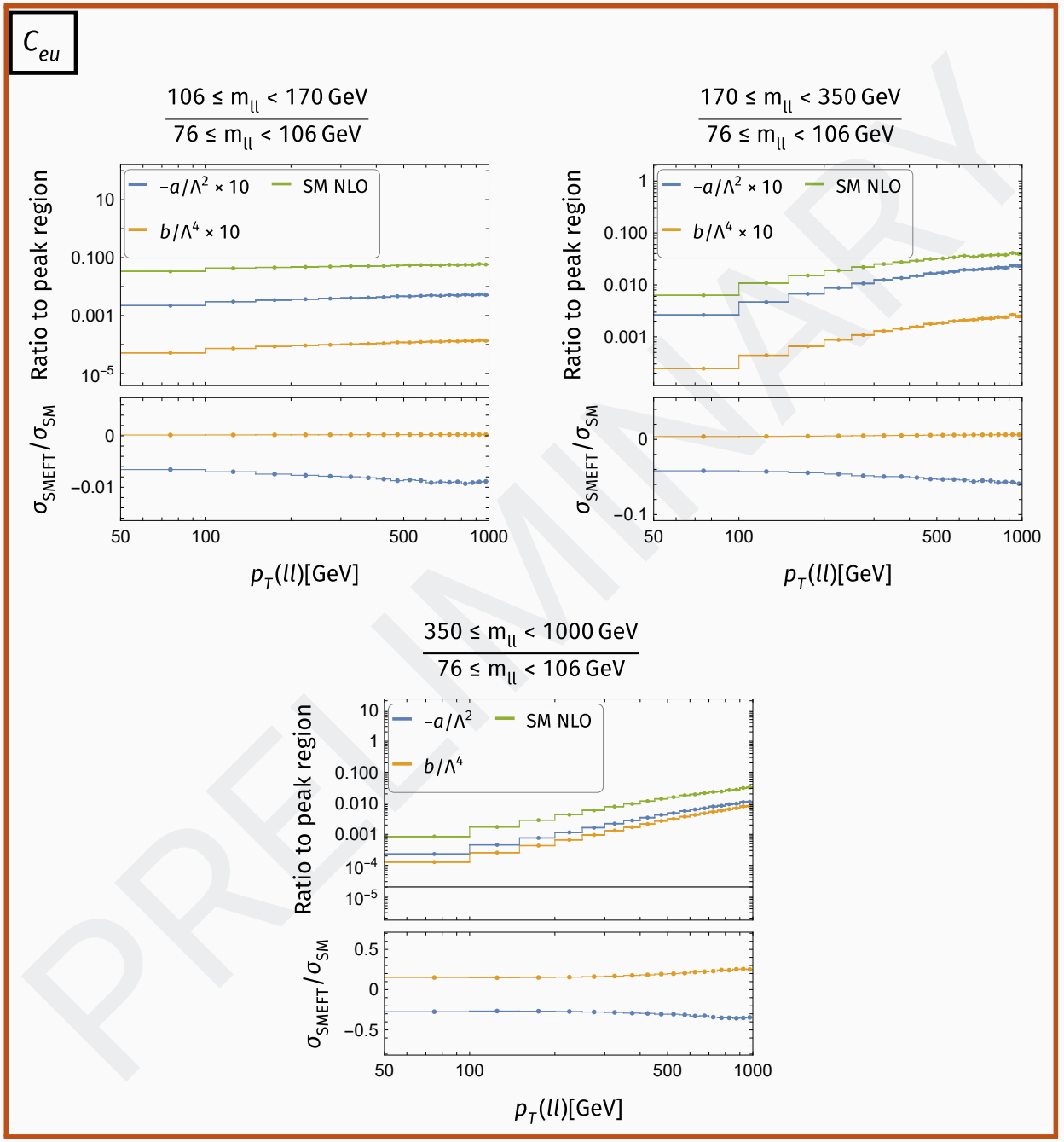

Impact of dim-8 terms $\psi^4 D^2$-type

- p_T bins: $50\ \mathrm{GeV}$ constant bin widths
- Smaller corrections to the ratio than dim-6
- Slower increase than $\psi^4 G$-type as p_T goes higher, but faster than dim-6

$C^{(1)}_{e^2u^2D^2}$

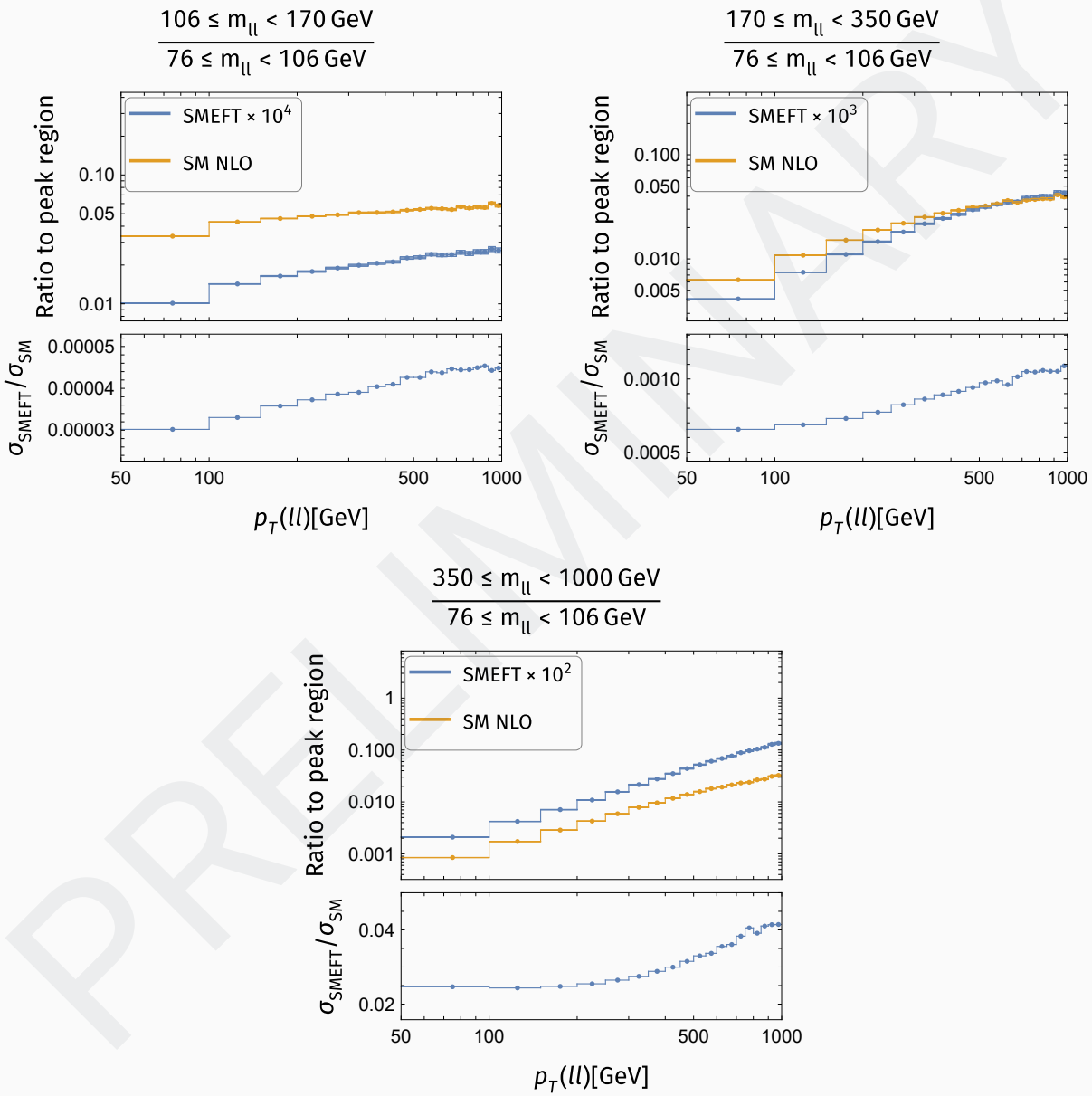

Impact of dim-8 terms $\psi^4 G$-type

- p_T bins: 50 GeV constant bin widths
- Smaller corrections to the ratio than dim-6
- Fastest increase as p_T goes higher

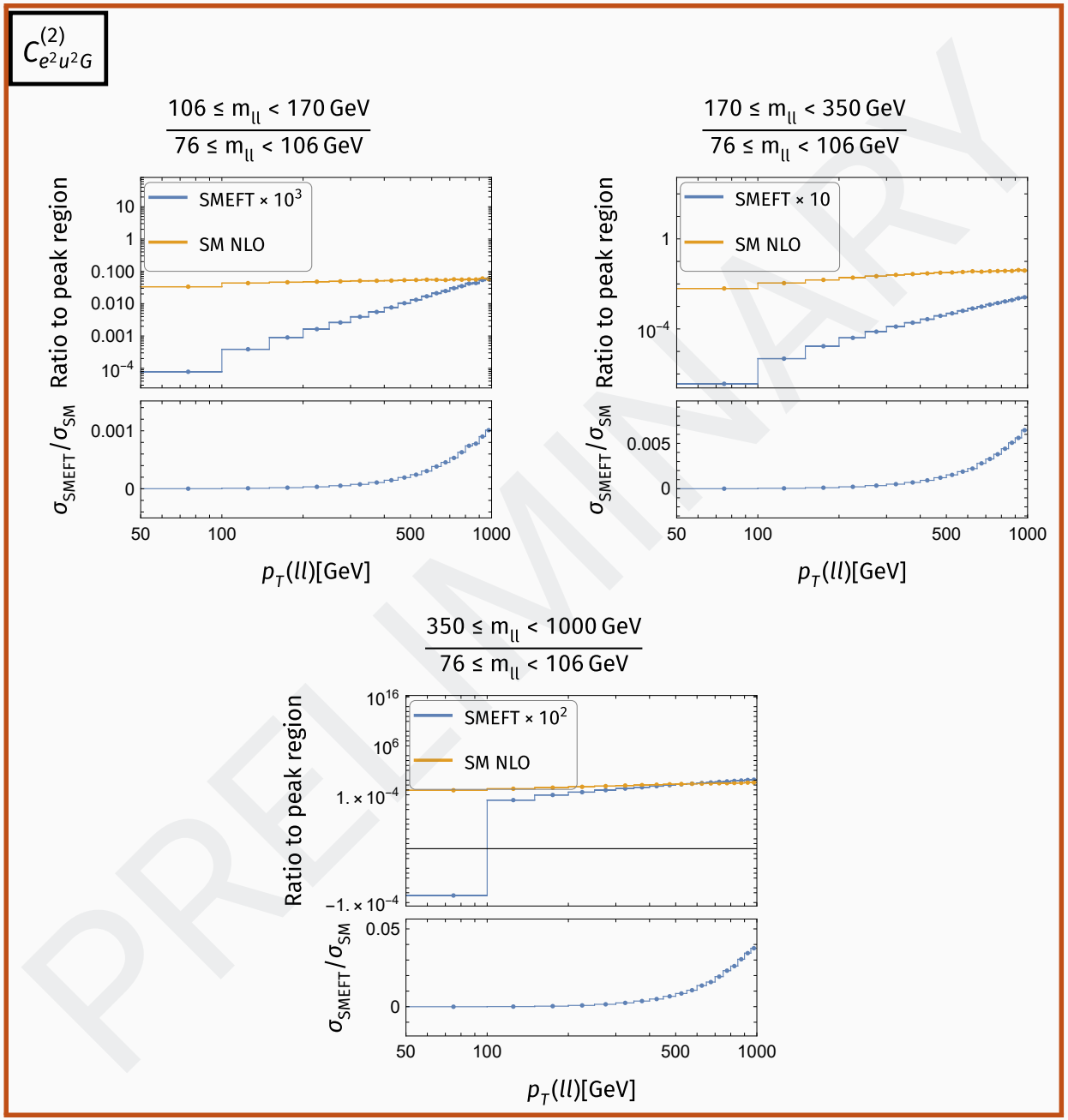

Single-coupling fits

- Fit with CMS data
- Experimental error matrix;

  CMS-PAS-SMP-20-003

  NNPDF 3.1 PDF errors;

  SM NLO QCD +

  LO SMEFT corrections

  for scale variation errors
- Only includes bins with $p_T \geq 52$ GeV

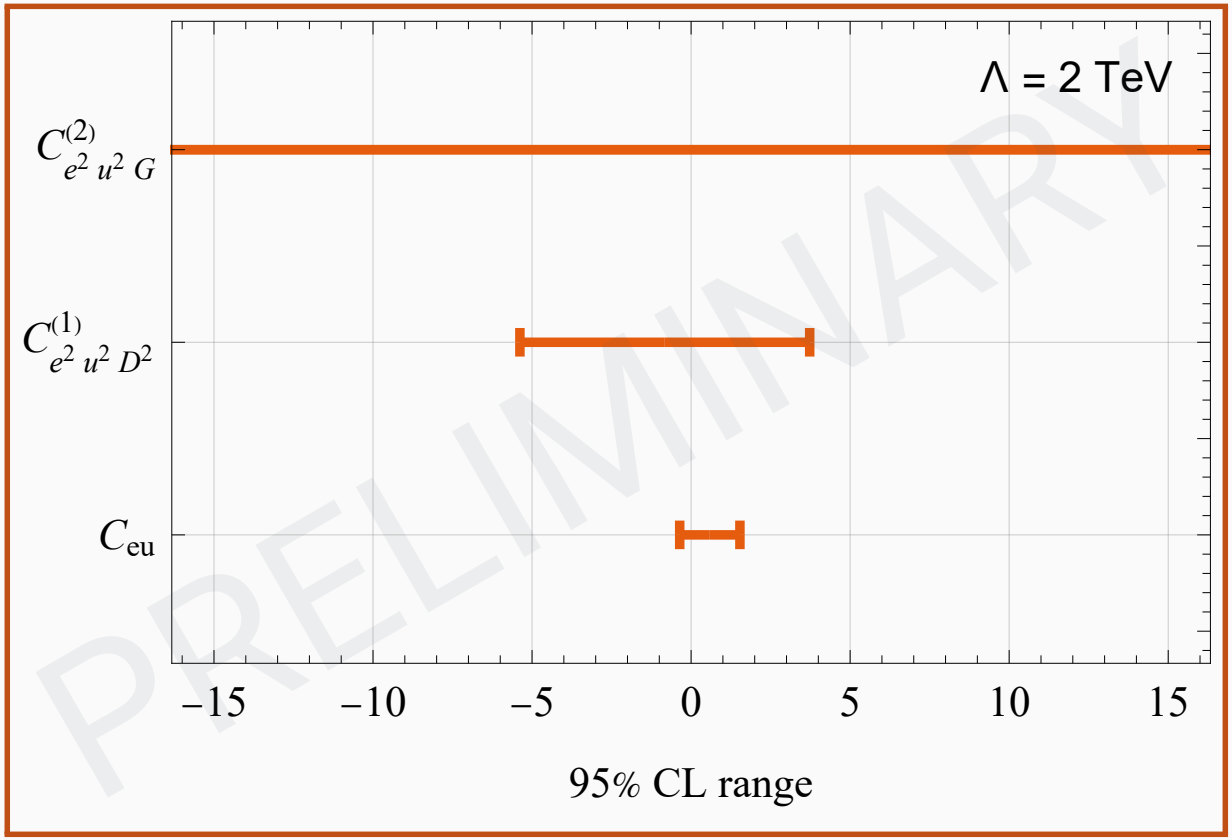

- effective scale $\gtrsim 1$ TeV $\Rightarrow |C_6| \leq 4, |C_8| \leq 16$

MULTI-COUPLING FITS Enabling 2 operators

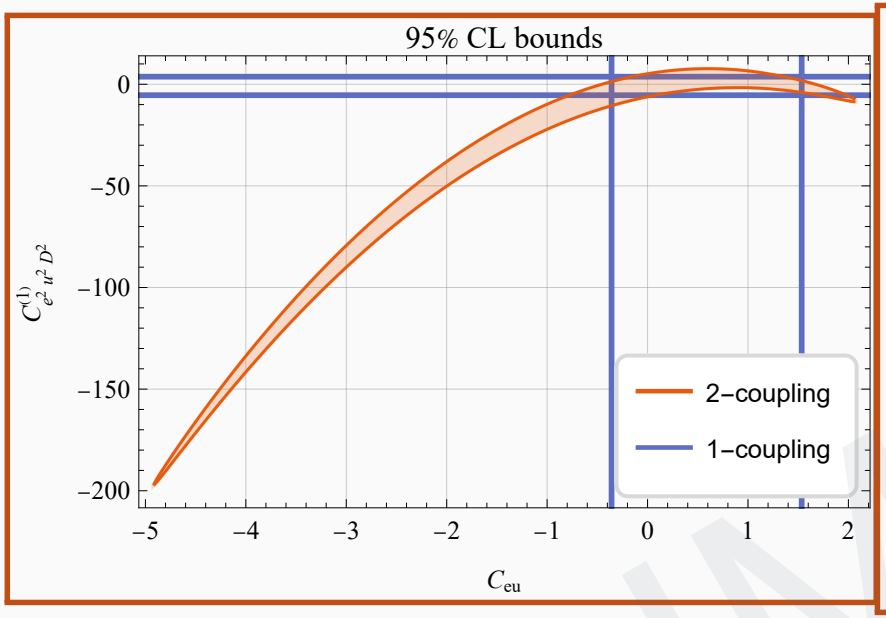

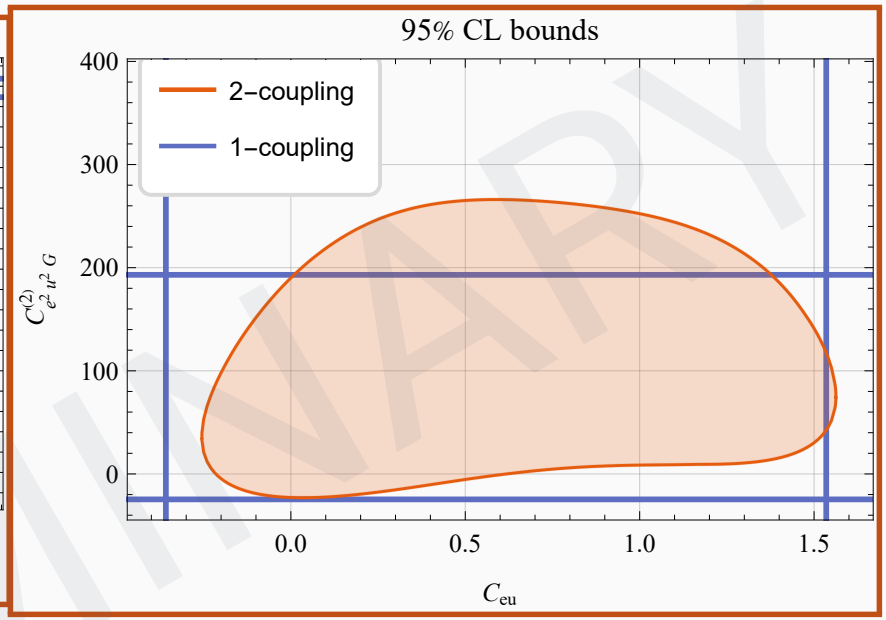

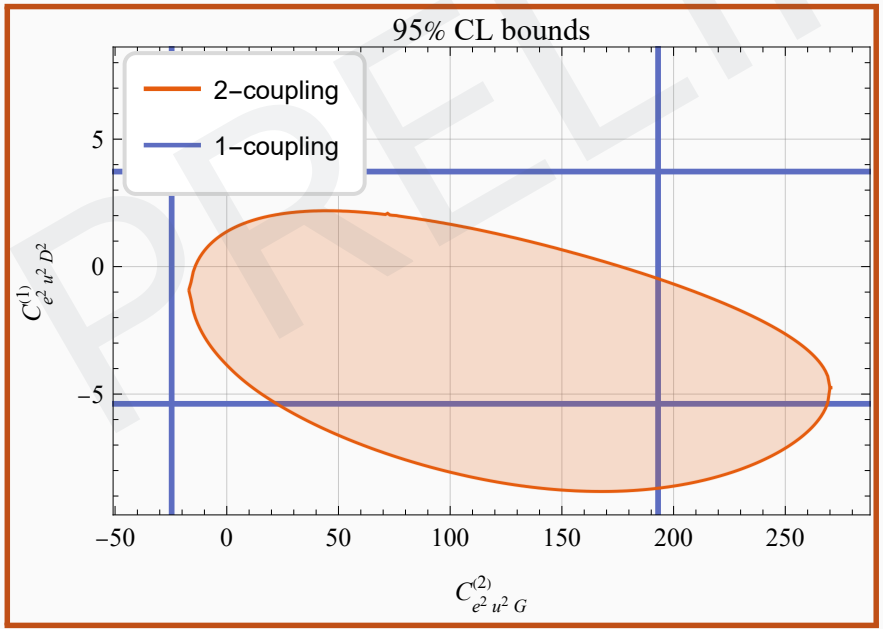

MULTI-COUPLING FITS Enabling 2 operators

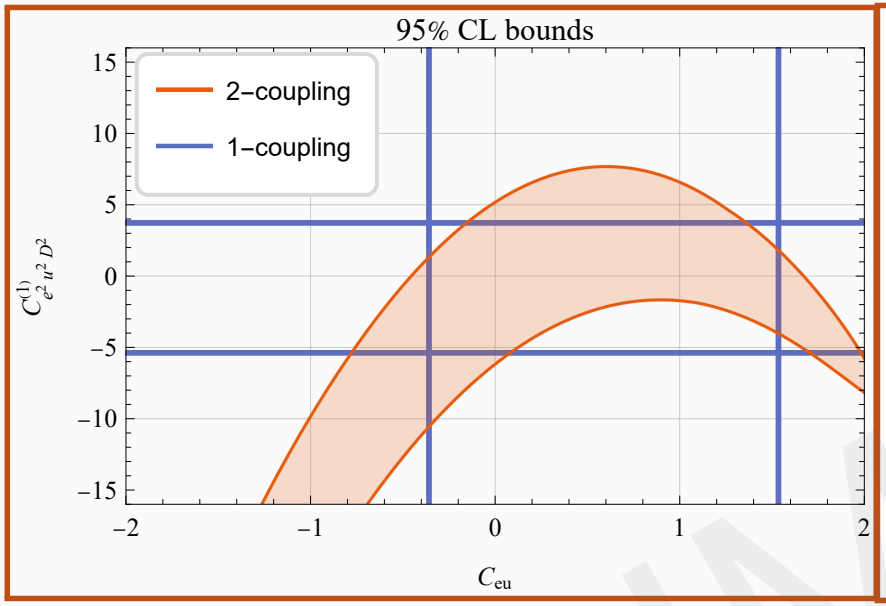

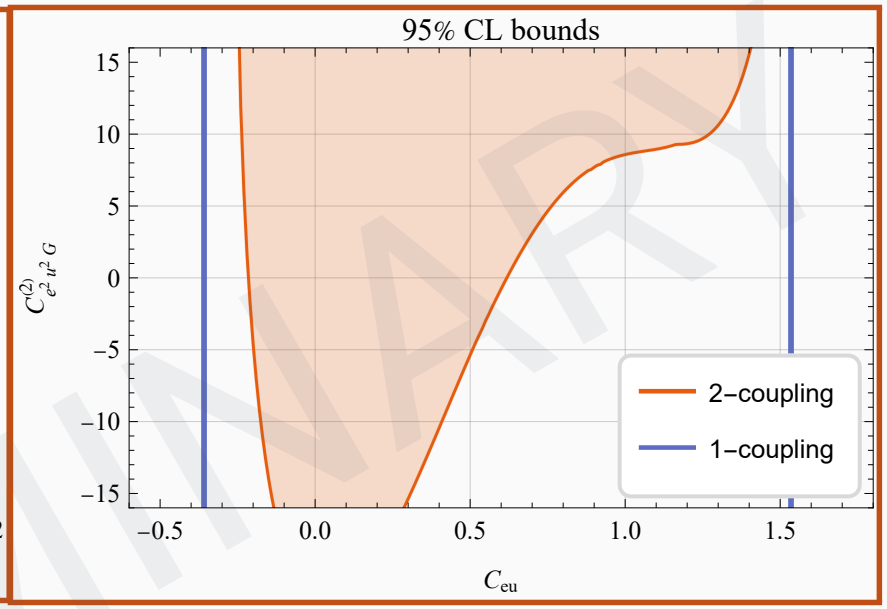

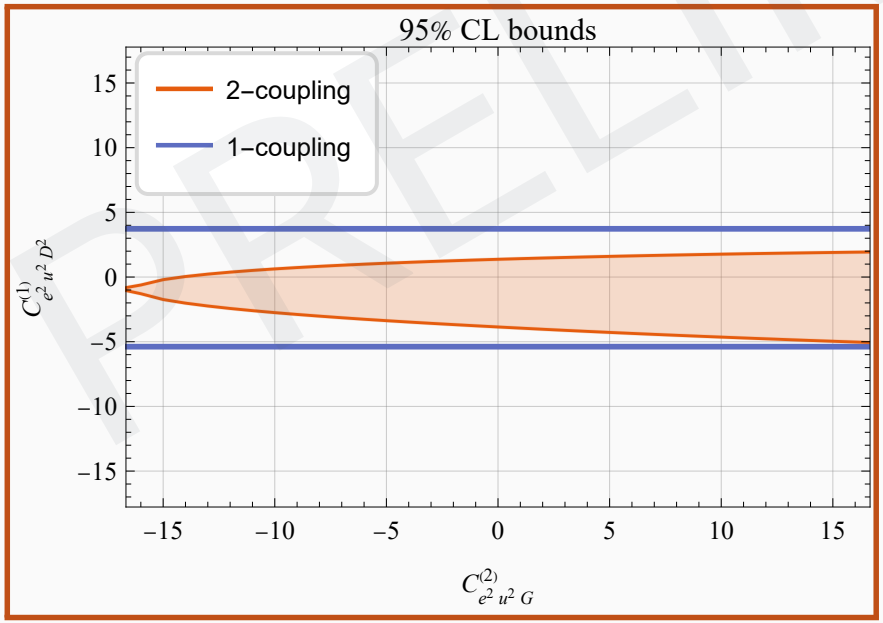

- effective scale $\gtrsim 1\ \mathrm{TeV}$

  $\Rightarrow |C_6| \leq 4, |C_8| \leq 16$

MULTI-COUPLING FITS Enabling 2 or 3 operators

Wilson coefficient	Single coupling	Marginalized	Marginalized*
C_{eu} & $C^{(1)}_{e^2u^2D^2}$			
C_{eu}	$[-0.358, 1.53]$	$[-4.12, 1.72]$	$[-1.42, 1.43]$
$C^{(1)}_{e^2u^2D^2}$	$[-5.38, 3.73]$	$[-122., 53.7]$	$[-15.6, 8.03]$
C_{eu} & $C^{(2)}_{e^2u^2G}$			
C_{eu}	$[-0.358, 1.53]$	$[-0.197, 1.40]$	$[-0.581, 1.43]$
$C^{(2)}_{e^2u^2G}$	$[-24.7, 193.]$	$[-7.05, 231.]$	$[-14.6, 16.0]$
all 3 operators			
C_{eu}	$[-0.358, 1.53]$	$[-4.57, 2.00]$	$[-1.41, 1.44]$
$C^{(1)}_{e^2u^2D^2}$	$[-5.38, 3.73]$	$[-155., 69.6]$	$[-15.5, 7.94]$
$C^{(2)}_{e^2u^2G}$	$[-24.7, 193.]$	$[-5.95, 250.]$	$[-15.1, 16.0]$

- $C^{(2)}_{e^2u^2G}$ does not change the bounds on C_{eu} very much
- $C^{(1)}_{e^2u^2D^2}$ changes the bounds on C_{eu} by a lot

Marginalized*: effective scale constraint ($\gtrsim 1$ TeV) on dim-8 operators

Dilepton mass-dependent p_T spectra with HL-LHC pseudo-data

Generation of pseudo-data

- m_{ll} bins: **Panico, Ricci, and Wulzer 2021**

  $[300, 360, 450, 600, 800, 1100, 1500, 2000, 2600]$
- p_T bins:
  - Assuming all stat. errors $< 5\%$, coarser binning

m_{ll}/GeV	p_T/GeV bins
$300 - 360$	$[100, 110, 120, 130, 140, 150, 160, 170, 180, 190, 200, 210, 220, 230, 250, 270, 290, 310, 330, 360, 380, 410, 440, 490, 570, 7000]$
$360 - 450$	$[100, 110, 120, 130, 140, 150, 160, 170, 180, 200, 230, 250, 270, 290, 310, 330, 350, 370, 400, 440, 490, 580, 7000]$
$450 - 600$	$[100, 110, 120, 130, 140, 150, 160, 170, 180, 190, 210, 230, 250, 270, 290, 320, 340, 360, 390, 430, 480, 580, 7000]$
$600 - 800$	$[100, 110, 120, 130, 150, 170, 200, 220, 250, 290, 320, 360, 420, 520, 7000]$
$800 - 1100$	$[100, 110, 120, 150, 170, 200, 230, 270, 330, 430, 7000]$
$1100 - 1500$	$[100, 200, 290, 7000]$
$1500 - 2000$	$[100, 7000]$
$2000 - 2600$	$[100, 7000]$

Generation of pseudo-data

- m_{ll} bins:

  $[300, 360, 450, 600, 800, 1100, 1500, 2000, 2600]$
- p_T bins:
  - Assuming all stat. errors $< 5\%$, coarser binning
  - Assuming all stat. errors $< 10\%$, finer binning

m_{ll}/GeV	p_T bins/GeV
$300 - 360$	$[100, 110, 120, 130, 140, 150, 160, 170, 180, 190, 200, 210, 220, 230, 250, 270, 290, 310, 330, 350, 370, 400, 420, 440, 470, 500, 530, 560, 600, 660, 760, 7000]$
$360 - 450$	$[100, 110, 120, 130, 140, 150, 160, 170, 180, 190, 200, 210, 220, 240, 260, 290, 310, 330, 350, 370, 390, 410, 440, 470, 500, 530, 560, 610, 670, 770, 7000]$
$450 - 600$	$[100, 110, 120, 130, 140, 150, 160, 190, 210, 230, 250, 270, 290, 320, 340, 370, 390, 420, 460, 490, 520, 550, 580, 620, 680, 780, 7000]$
$600 - 800$	$[100, 110, 120, 130, 150, 170, 200, 220, 240, 260, 280, 310, 340, 380, 410, 440, 470, 510, 550, 620, 730, 7000]$
$800 - 1100$	$[100, 110, 120, 140, 160, 180, 200, 220, 250, 270, 300, 330, 360, 410, 460, 540, 660, 7000]$
$1100 - 1500$	$[100, 130, 160, 190, 230, 270, 320, 400, 520, 7000]$
$1500 - 2000$	$[100, 210, 330, 7000]$
$2000 - 2600$	$[100, 7000]$

Generation of pseudo-data

- m_{ll} bins:

  $[300, 360, 450, 600, 800, 1100, 1500, 2000, 2600]$
- p_T bins:
  - Assuming all stat. errors $< 5\%$, coarser binning
  - Assuming all stat. errors $< 10\%$, finer binning
- assume 1% uncorrelated sys. error and 2% correlated sys. error

2-COUPLING FITS $C^{(1)}_{e^2u^2D^2}$

Fit to data with <5% error

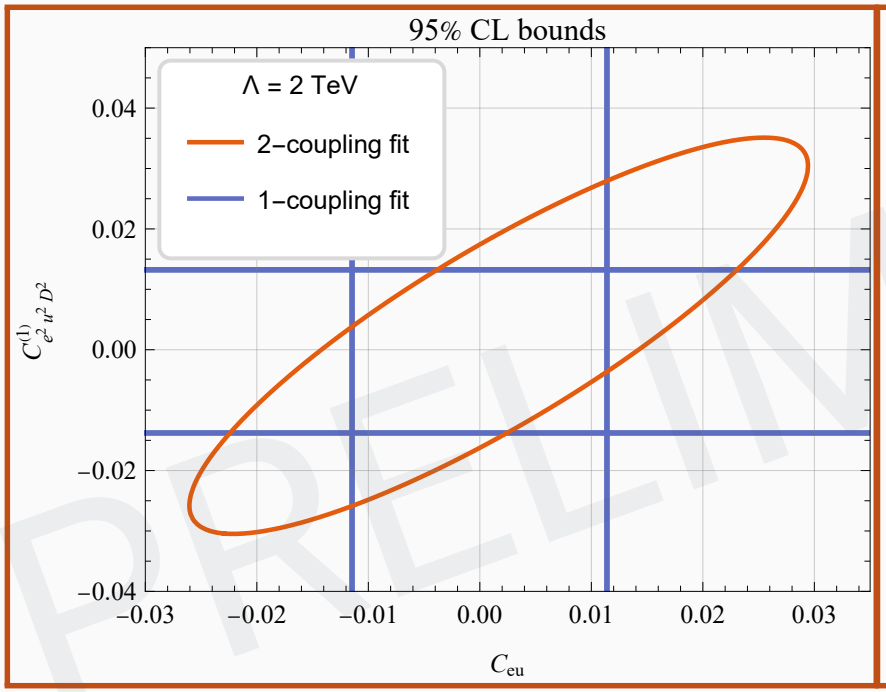

Fit to data with <10% error

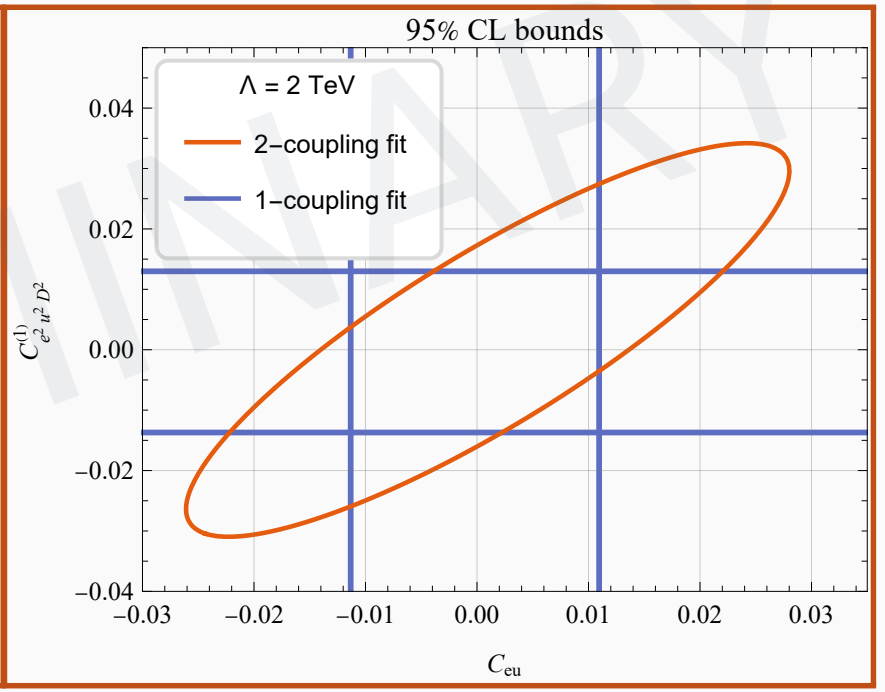

- C_{eu} & $C^{(1)}_{e^2u^2D^2}$ are highly correlated
- need other experiments to independently constrain C_{eu}
  i.e. low-energy PVES experiments such as SoLID
- Tighter bounds from “<10%” dataset

2-COUPLING FITS $C^{(2)}_{e^2u^2G}$

Fit to data with <5% error

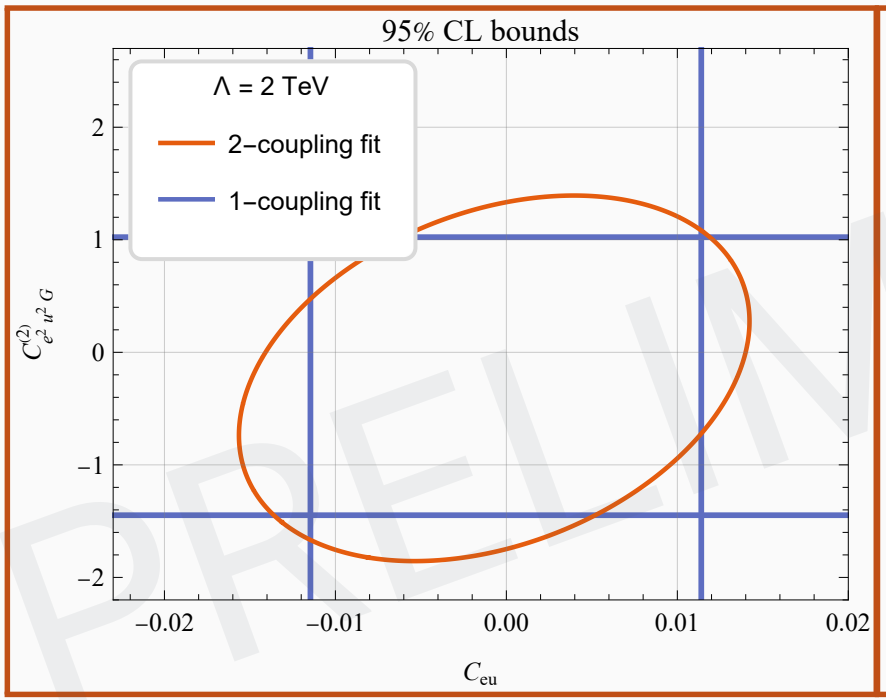

Fit to data with <10% error

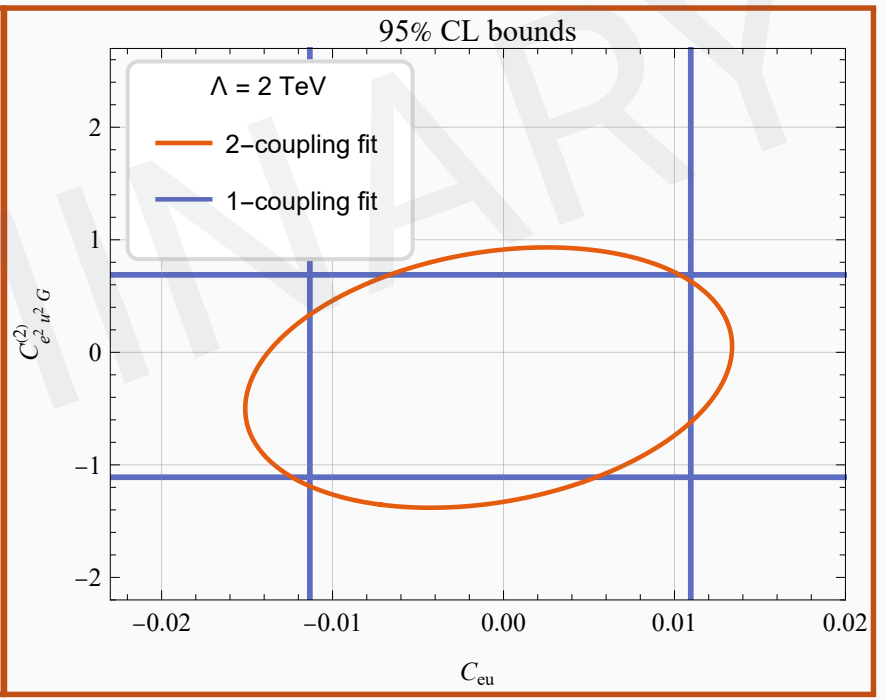

- C_{eu} & $C^{(2)}_{e^2u^2G}$ are almost uncorrelated
- Can independently determine C_{eu} with m_{ll} and $C^{(2)}_{e^2u^2G}$ with p_T spectra
- Tighter bounds from “<10%” dataset

3-COUPLING FITS project to 2-d

Fit to data with <5% error

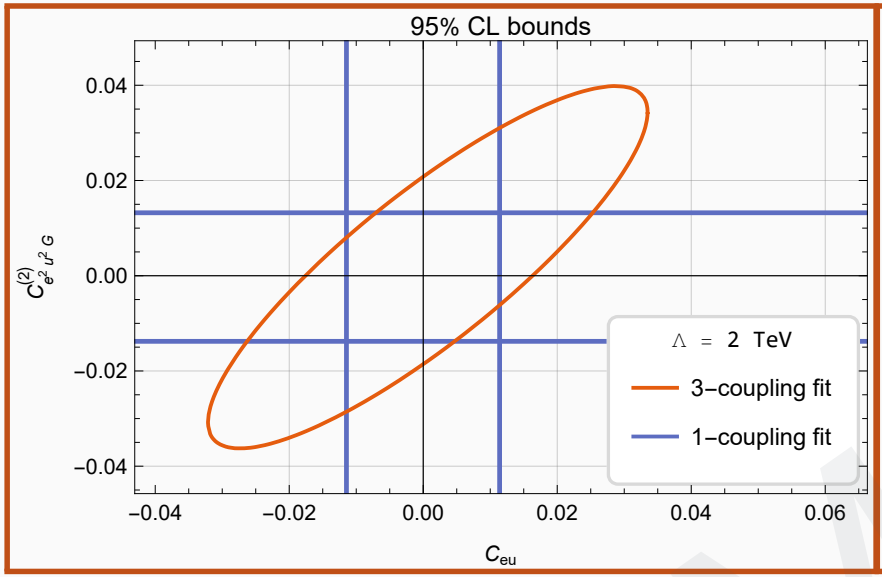

Fit to data with <10% error

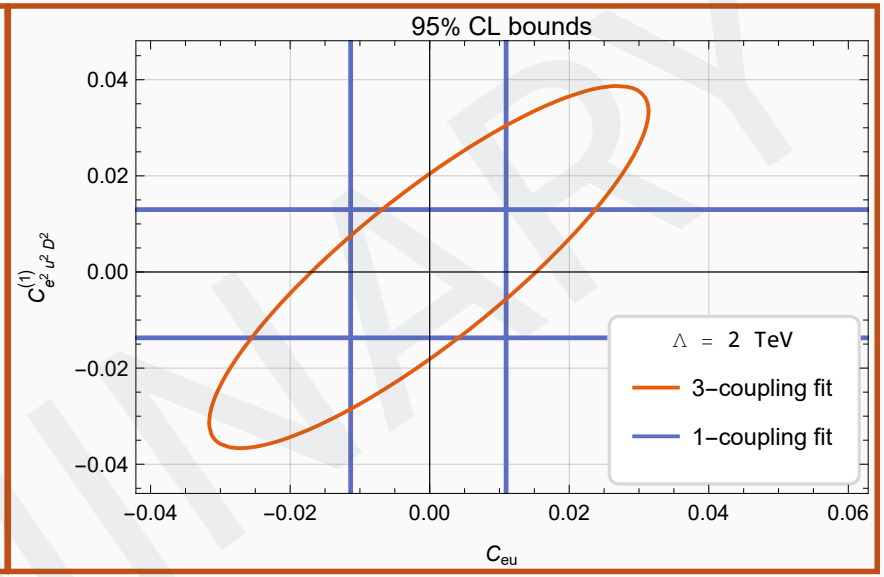

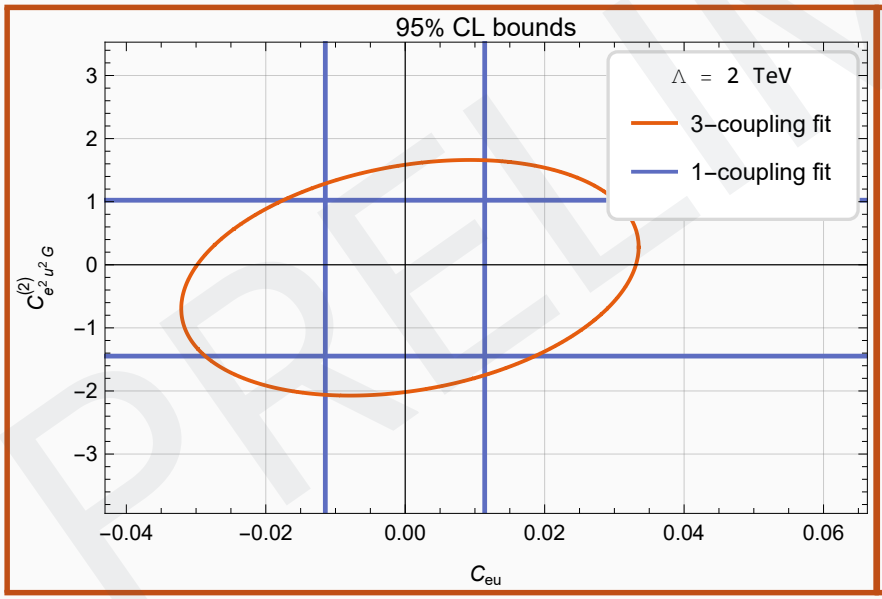

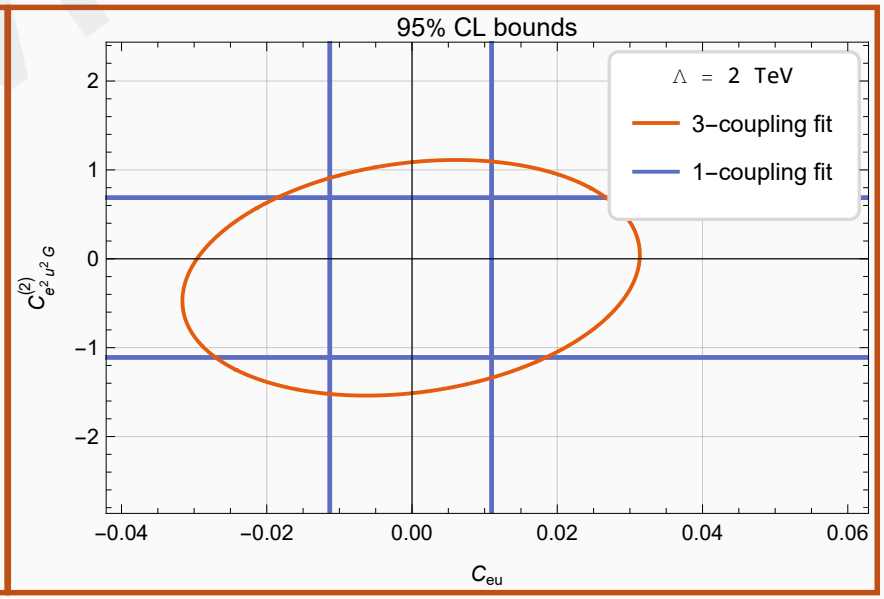

3-COUPLING FITS project to 2-d

Fit to data with <5% error

Fit to data with <10% error

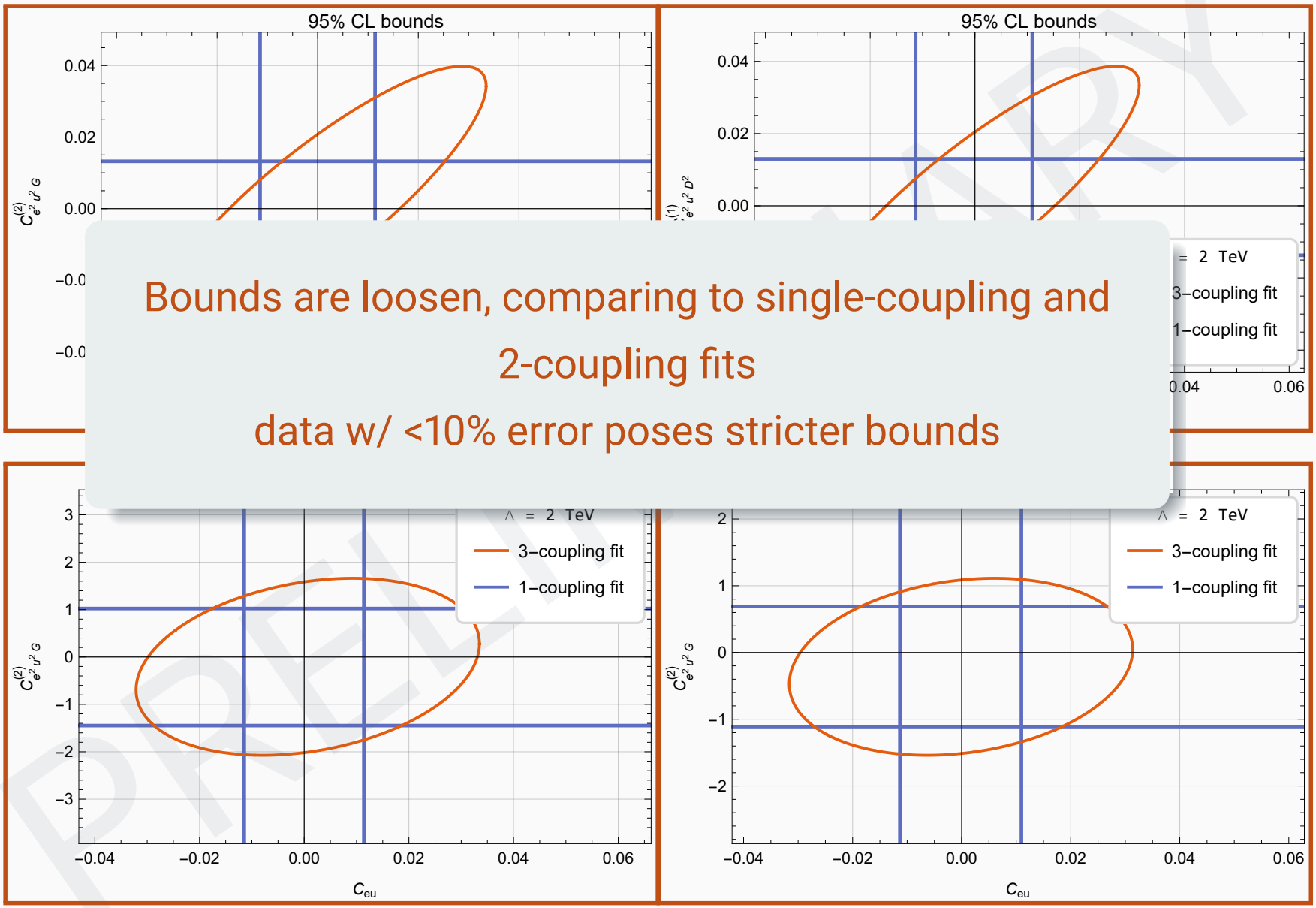

Bounds are loosen, comparing to single-coupling and 2-coupling fits

data w/ <10% error poses stricter bounds

Summary

Summary

- Included $\mathcal{O}(1/\Lambda^4)$ effects
- Analyzed scaling in high energy limit: justified to only include operators with $\mathcal{O}(s/\Lambda^2)$ or $\mathcal{O}(s^2/\Lambda^4)$ scaling
- Effects of those dim-8 operators with highest scaling can not be neglected
- Study on Drell-Yan m_{ll} and p_T spectra both indicate strong correlation between C_{eu} & $C^{(1)}_{e^2u^2D^2}$
- Study on Drell-Yan p_T spectra reveals nearly no correlation between C_{eu} & $C^{(2)}_{e^2u^2G}$
- C_{eu} & $C^{(1)}_{e^2u^2D^2}$: flat direction; calls for other experiments such as PVES

Thanks for your attention!

Backup